www.czasopisma.pan.pl PAN www.journals.pan.pl

Acta Geologica Polonica, Vol. 69 (2019), No. 1, pp. 143–160
DOI: 10.24425/agp.2019.126437

Magma mingling textures in granitic rocks of the eastern part of the Strzegom-Sobótka Massif (Polish Sudetes)

JUSTYNA DOMAŃSKA-SIUDA and BOGUSŁAW BAGIŃSKI

Faculty of Geology, University of Warsaw, al. Żwirki i Wigury 93, 02-089 Warszawa, Poland.
Corresponding author: j.domanska@uw.edu.pl

ABSTRACT:

Domańska-Siuda, J. and Bagiński, B. 2019. Magma mingling textures in granitic rocks of the eastern part of the Strzegom-Sobótka Massif (Polish Sudetes). *Acta Geologica Polonica*, **69** (1), 143–160. Warszawa.

Many granitic intrusions display evidence of magma mixing processes. The interaction of melts of contrasting composition may play a significant role during their generation and evolution. The Strzegom-Sobótka massif (SSM), located in the Sudetes (SW Poland) in the north-eastern part of the Bohemian Massif of the Central European Variscides, exhibits significant evidence of magma mingling on the macro- and micro-scales. The massif is a composite intrusion, with four main varieties: hornblende-biotite granite (with negligible amount of hornblende) and biotite granite in the western part, and two-mica granite and biotite granodiorite in the eastern part. Field evidence for magma mingling is easily found in the biotite granodiorite, where dark enclaves with tonalitic composition occur. Enclaves range from a few centimeters to half a meter in size, and from ellipsoidal to rounded in shape. They occur individually and in homogeneous swarms. The mixing textures in the enclaves include fine-grained texture, acicular apatite, rounded plagioclase xenocrysts, ocellar quartz and blade-shaped biotite. The most interesting feature of the enclaves is the presence of numerous monazite-(Ce) crystals, including unusually large crystals (up to 500 μm) which have grown close to the boundaries between granodiorite and enclaves. The crystallization of numerous monazite grains may therefore be another, previously undescribed, form of textural evidence for interaction between two contrasting magmas. The textures and microtextures may indicate that the enclaves represent globules of hybrid magma formed by mingling with a more felsic host melt. Chemical dating of the monazite yielded an age of 297±11 Ma.

Key words: Strzegom-Sobótka massif; Granite; Enclave; Variscides; Magma mixing; Magma mingling; Textures; Monazite-(Ce) crystals.

INTRODUCTION

Mafic magmatic enclaves (MMEs; Barbarin 1988, 2005), also termed mafic microgranular enclaves (Didier 1973; Didier and Barbarin 1991; Poli and Tommasini 1991) or microgranular magmatic enclaves, are common in calc-alkaline granitoid plutons (Bacon 1986; Didier and Barbarin 1991), and are also abundant in most Sudetic Variscan intrusions (Gerdes *et al.* 2000; Janoušek *et al.* 2000, 2004; Słaby and Martin 2008, Słaby *et al.* 2008; Pietranik and Koepke 2014; Michel *et al.* 2016). Their presence in felsic plutons is considered important evidence of mafic-felsic melt interactions and potentially gives us valuable information on the origin and evolution of the host magma and its influence on the composition of the pluton, mineral compositions and growth textures. The enclaves may also preserve important information on the nature of parental magmas (Didier 1973; Didier and Barbarin 1991; Vernon 1984, 1991; Castro *et al.* 1990; Barbarin and Didier 1991; Hibbard 1991; Orsini *et al.* 1991; Wiebe *et al.* 1997; Barbarin 2005; Vernon 2010).

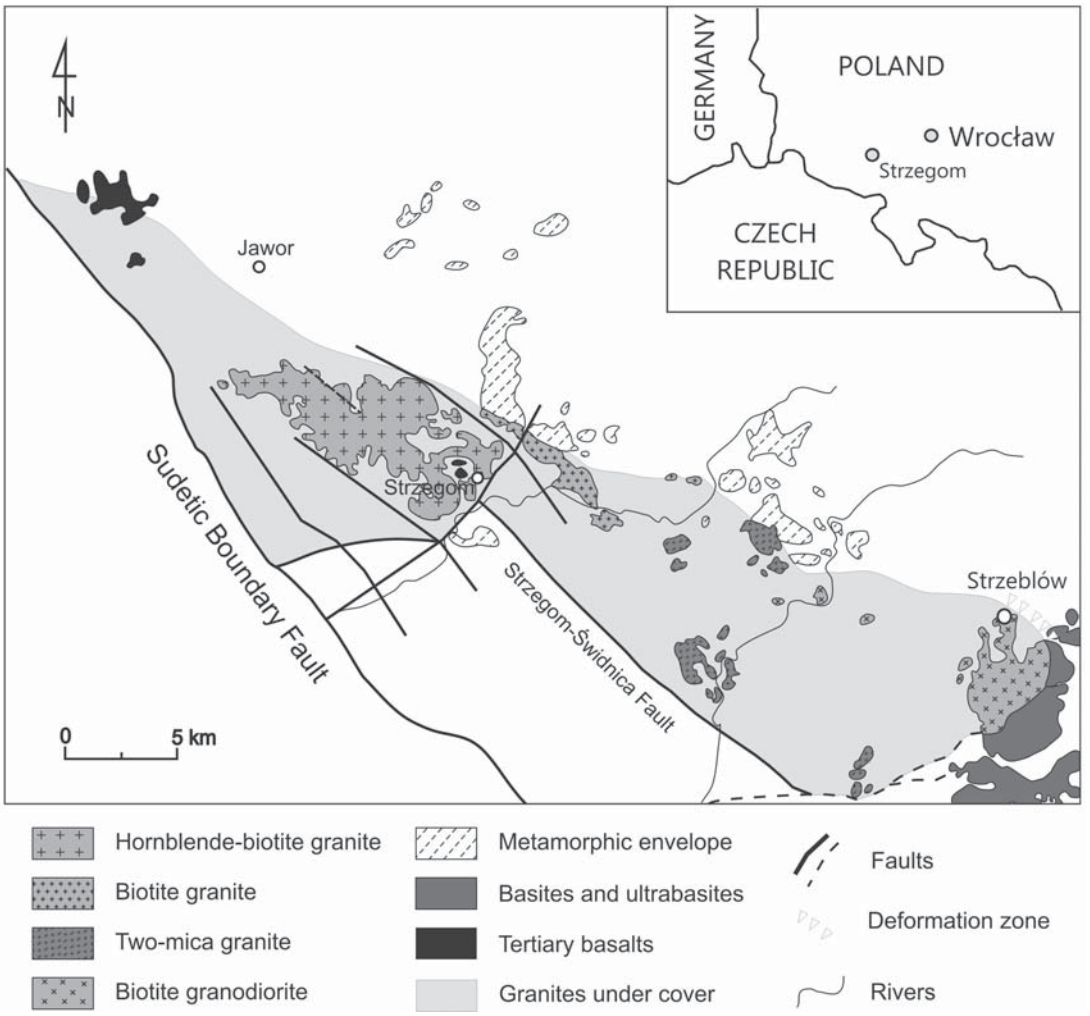

Text-fig. 1. Geological sketch map of the Strzegom-Sobótka massif, with the granitoid varieties distinguished (modified after Majerowicz 1972 and Puziewicz 1990). The location of the Strzeblów quarry is marked. The triangles mark the deformation zone bordering the intrusion to the east

This paper presents new petrographical data as well as field observations and age estimates of the biotite granodiorites and their enclaves from the eastern part of the Strzegom-Sobótka massif. We describe in detail a group of enclaves belonging to one swarm and the textures that occur in the contact zone between them and host granodiorite. We also report on monazites of unusually large size (up to 500 μm) which grew at the interface between magmas of contrasting composition, their growth apparently being promoted, or facilitated, by interaction between the magmas. The presence of numerous grains of monazite may indicate the mobility of not only the main elements, but also the rare earth elements, caused by the interaction of compositionally different melts.

GEOLOGICAL SETTING

The Variscan granites of the Sudetes, SW Poland, show two distinct age groups, at ~340–330 Ma and 320–295 Ma (Mazur *et al.* 2007 and references therein). Emplacement of the older granites was related to the main stage of nappe stacking within the Central European Variscides and the granites are thought to have formed by dehydration melting at mid-crustal levels through thermal relaxation of overthickened Variscan crust (e.g., Franke 2000). The younger magmatic event was post-tectonic and resulted in more voluminous granitic plutons, mainly of peraluminous composition. The plutons were locally accompanied by contemporaneous mafic to interme-

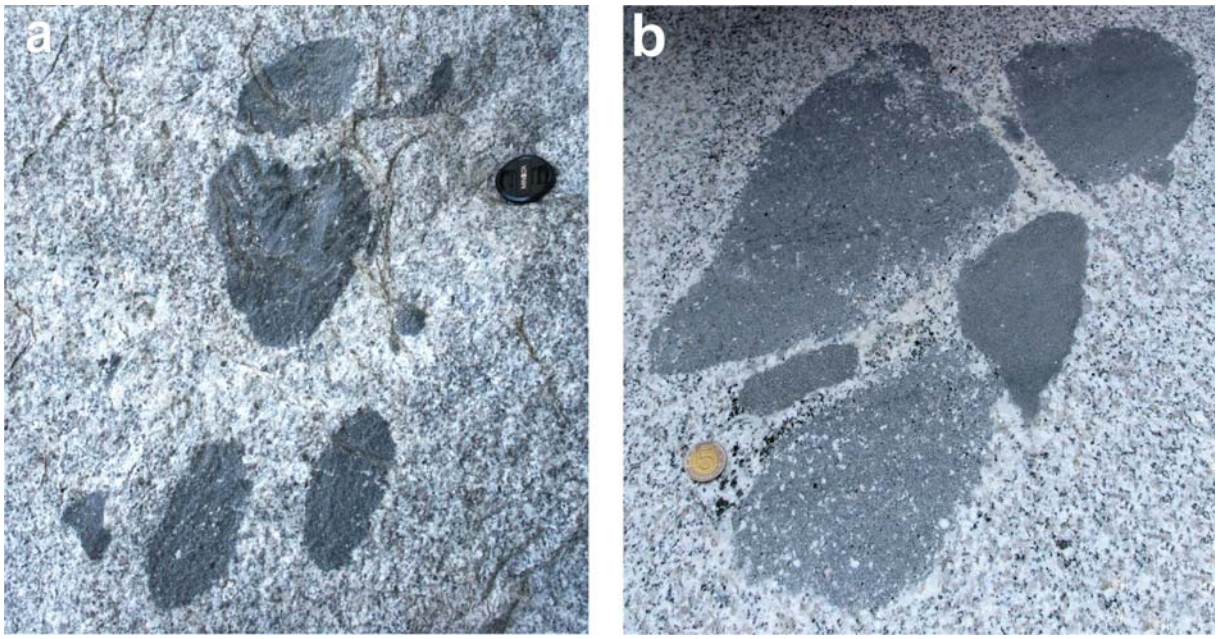

Text-fig. 2. Field photographs showing the variability in enclave characteristics. **a** – Microstructurally and compositionally similar enclaves in the biotite granodiorite. Note the different shapes and the common orientation of the enclaves. **b** – Mixed enclave swarm in the biotite granodiorite showing distinct textural/compositional types, suggesting different degrees of hybridization with the host rock

diate magmatism, in the form of tonalitic to lamprophyric dykes and mafic magmatic enclaves and were broadly associated with mafic to silicic volcanism in intermontane basins (Kryza and Awdankiewicz 2012; Awdankiewicz *et al.* 2014; Turniak *et al.* 2014). The younger phase of magmatism had a clear input of material from the lithospheric mantle, perhaps related to lithospheric extension following the end of Variscan convergence (Henk 1997; Pietranik and Wright 2008; Turniak *et al.* 2014). Most of the granitic bodies are composite plutons that crystallized from melts derived from many sources (e.g., Pin *et al.* 1989; Gerdes *et al.* 2000; Domańska and Słaby 2004; Domańska-Siuda and Słaby 2005; Słaby and Götze 2004; Słaby and Martin 2008; Słaby *et al.* 2008; Pietranik and Koepke 2009; Pietranik and Koepke 2014; Lisowiec *et al.* 2015; Oberc-Dziedzic *et al.* 2013; Žák *et al.* 2013; Laurent *et al.* 2014; Jokubauskas *et al.* 2017; Birski *et al.* 2018; Domańska-Siuda *et al.* 2019).

The Strzegom-Sobótka Massif is the largest granite pluton within the central part of the Fore-Sudetic block (the NE part of the Variscan belt), about 50 km southwest of the city of Wrocław (Text-fig. 1). Elongated SE-NW and approximately 50 km long, the massif has a maximum width of ~12 km. The Strzegom-Świdnica fault divides it into eastern and western parts. On the northwestern side, the intrusion borders on the Sudetic Boundary Fault, separating it from the metamorphic rocks of the Kaczawskie Mountains. This Tertiary fault separates the mountainous part of the Sudetes in the southwest from the Fore-Sudetic Block in the northeast.

The Góry Sowie Massif borders the Strzegom-Sobótka intrusion on the southeast. The massif is mainly composed of gneisses and migmatites, with subordinate mafic and ultramafic rocks and small granulitic bodies. The protoliths have been dated as Late Proterozoic–Early Palaeozoic (Olivier *et al.* 1993; Brueckner *et al.* 1996; Kröner and Hegner 1998; Kryza and Fanning 2004). No contacts between the granitoids and gneisses are seen at outcrop. On the eastern side, the intrusion is in contact with mafic and ultramafic rocks (gabbros, serpentinites, amphibolites and metavolcanics) of the Śleża Massif, part of the Central Sudetic Ophiolite. These rocks were dated as of Late Devonian–Early Carboniferous age (Pin *et al.* 1988; Oliver *et al.* 1993; Dubińska *et al.* 2004; Kryza and Pin 2010). On the southeast and northern sides, the intrusion is accompanied by Palaeozoic rocks (micaceous, sericitic, chlorite and quartzitic schists, locally intercalated with dolomite and greywacke-argillaceous shales, diabases and

quartzites), which are buried under Cenozoic deposits (Majerowicz 1972).

The intrusion is composed of few main lithological types: hornblende-biotite granite (with negligible amount of hornblende) and biotite granite, both occurring mainly in the western part, and two-mica granite and biotite granodiorite, occurring mainly in the eastern part (Kural and Morawski 1968; Majerowicz 1972; Maciejewski and Morawski 1975; Puziewicz 1990) (Text-fig. 1). We focus here on the biotite granodiorite in the eastern part of the massif, which is exposed mainly in quarries but also forms small, isolated outcrops. Little is known about the form of the granodiorite; from the overall shape of the outcrop it is perhaps boss-like. The biotite granodiorite contains microgranular enclaves with mainly tonalitic composition (Text-fig. 2).

The biotite granodiorite has been dated using the Rb-Sr whole rock method, with an age close to 280 Ma (Pin *et al.* 1988, 1989) and an initial $^{87}Sr/^{86}Sr$ ratio of 0.7058. A Pb evaporation zircon age for the biotite granodiorite is 308.4 ± 1.7 Ma, which may be interpreted as the time of zircon crystallization from the melt (Turniak *et al.* 2005). K-Ar dating of biotite gave ages of 308.8 ± 4.6 and 305.5 ± 4.3 Ma (Turniak *et al.* 2007). U-Pb zircon dating for the biotite granodiorite gave ages ranging between 301.9 ± 3.6 and 297.9 ± 3.7 Ma (Turniak *et al.* 2014). Chemical dating of monazite obtained for the biotite granodiorite (Chwałków quarry) gave an age of 300.2±11.2 Ma (Turniak *et al.* 2011). Zircon saturation temperatures based on whole-rock compositions are in the range 702–787°C, taken to be the interval over which magmatic differentiation occurred (Turniak *et al.* 2014).

The depth at which the granodiorite crystallized is poorly constrained. Szuszkiewicz (2007) estimated 3–5 km for monzogranites from the western part of the Strzegom-Sobótka massif, perhaps indicative that the granodiorite also cooled at upper crustal levels.

ANALYTICAL METHODS

Samples were collected in the Strzeblów quarry (Text-fig. 1). Whole-rock chemical analyses were carried out in the ACME Analytical Laboratories Ltd. (Vancouver, Canada). Major and some trace elements were analysed using ICP-ES, rare earth elements using ICP-MS, according to procedures described on http://acmelab.com.

The chemical compositions of minerals were investigated using a Cameca SX-100 electron microprobe (WDS mode) in the Electron Microprobe Laboratory at the Inter-Institute Microanalytical Complex for Minerals and Synthetic Substances, Warsaw University, Poland. The following instrumental conditions were applied: a counting time of 10–20 s; an acceleration voltage of 15 kV and a beam current of 20 nA for major elements and those of 20–30 kV and 50 nA for trace elements. The following standards were used: albite (Na); diopside (Mg, Si, Ca); wollastonite (Si, Ca); orthoclase (K, Al); haematite (Fe); rhodochrosite (Mn); apatite (P, F); phlogopite (F); barite (S, Ba); rutile (Ti); zircon (Zr); synthetic strontium titanite (Sr); YAG (Y); end-member synthetic phosphates (XP_5O_{14}) for each REE; synthetic uraninite (U); synthetic thorianite (Th); crocoite (Pb); synthetic chromium(III) oxide, Cr_2O_3 (Cr); synthetic NiO (Ni) and tugtupite (Cl). The typical spot size ranged between 2–5 μm depending on the analysed mineral. Matrix correction was performed using the standard PAP procedure.

The analytical procedures used to obtain the highest quality data for monazite chemical dating were as follows: (1) An ordinary analysis was done at an accelerating voltage of 20 kV, with a beam current of 50 nA and a counting time (peak and background) of 600 s for Pb, 400 s for U, 200 s for Th. (2) A "trace" type of analysis was done at an accelerating voltage of 20 kV, with a beam current of 150 nA and a counting time (peak+background) of 600 s for Pb, 400 s for U, and 200 s for Th and Y**.** Only Th, Pb, U and Y were measured; the other components were treated as a matrix. The most important X-ray lines used for contents calculations were *M*β for U and Pb and *M*α for Th. The correction factor for U content was from Scherrer *et al.* (2000).

Dozens of grains were first mapped with the Σigma VP Zeiss FE-SEM equipped with two SDD type Bruker XFlash-10 EDS detectors to establish Y distribution within the crystals, and the most suitable crystals for further dating selected. The relative abundance of Y was determined from the interference-free YKα line. The maximum available 30kV acceleration voltage was used for the most effective generation of YKα, but the second largest 60 μm aperture was used to stay below the 25% dead time of the EDS signal processing unit. Six monazite grains were selected for chemical age determination.

Rock textures and crystal morphology were examined in thin sections by standard petrographic microscopy using a Nikon E-600 microscope and by backscattered electron (BSE) imaging on a JEOL 6380 at the Scanning Electron Microscope and Microanalysis Laboratory, Faculty of Geology, Warsaw University.

PETROGRAPHY AND GEOCHEMISTRY OF THE HOST BIOTITE GRANODIORITE AND MICROGRANULAR MAGMATIC ENCLAVES

Biotite granodiorite

The biotite granodiorite is light-grey, equigranular and slightly foliated, the foliation locally being accentuated by the presence of lens-shaped quartz aggregates. It is composed of plagioclase (36–48% modally), K-feldspar (20–25%), quartz (23–35%) and biotite (3–6%), with accessory zircon, apatite, allanite, monazite, xenotime and opaque minerals. The plagioclase forms subhedral to euhedral prisms, 0.5–1.0 cm long on average. Normal zoning is ubiquitous, from An_{46} in cores to An_6 in rims (Text-fig. 3a). The zoning can be continuous or discontinuous, locally oscillatory. Patchy zoning, especially in crystal cores, are also observed. K-feldspar and quartz form inclusions (Text-fig. 3b). Alkali feldspar forms mainly anhedral crystals, up to two cm across. It is microcline, commonly showing perthitic exsolution lamellae. Biotite inclusions are present. Quartz occurs as anhedral, interstitial grains showing weak shadowy extinction. It is sometimes broken into numerous subgrains and also forms mosaic aggregates.

Biotite forms anhedral flakes, discrete or in aggregates, and is strongly pleochroic from light straw yellow to dark red-brown. Some grains are partly chloritised. Zircon inclusions are common. The biotite has high ^{IV}Al (3.0 apfu) and 100.Fe*/(Fe*+Mg) ratios of 63–64. The opaque phases (ilmenite and pyrite) form inclusions in biotite or interstitial crystals. Zircon is less abundant than monazite, and shows rectangular, rounded or elongate forms up to 0.1 mm. Like monazite, it is present in biotite as inclusions and less often in plagioclase. Euhedral, prismatic crystals of apatite form inclusions, most commonly in biotite (Text-fig. 4a) and less often in feldspars and quartz. Allanite is less common and forms automor-

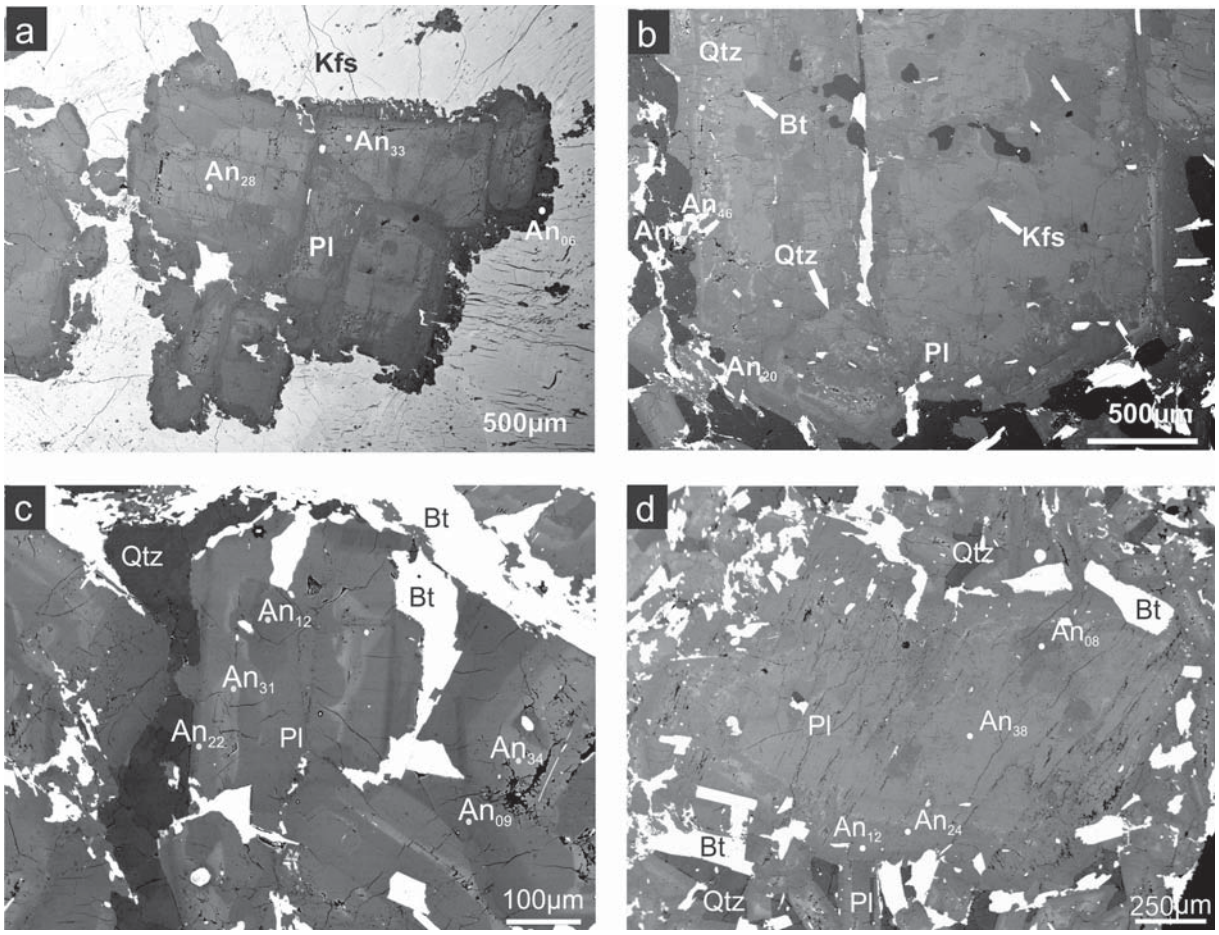

Text-fig. 3. BSE images of different type of plagioclase. **a –** Euhedral, normal zoning plagioclase (the biotite granodiorite). **b** – Euhedral, patchy zoning crystal of plagiocase with K-feldspar and quartz inclusions (the biotite granodiorite). **c** – Euhedral laths of plagioclase, building a groundmass of enclave. **d** – Plagioclase xenocryst inside enclave

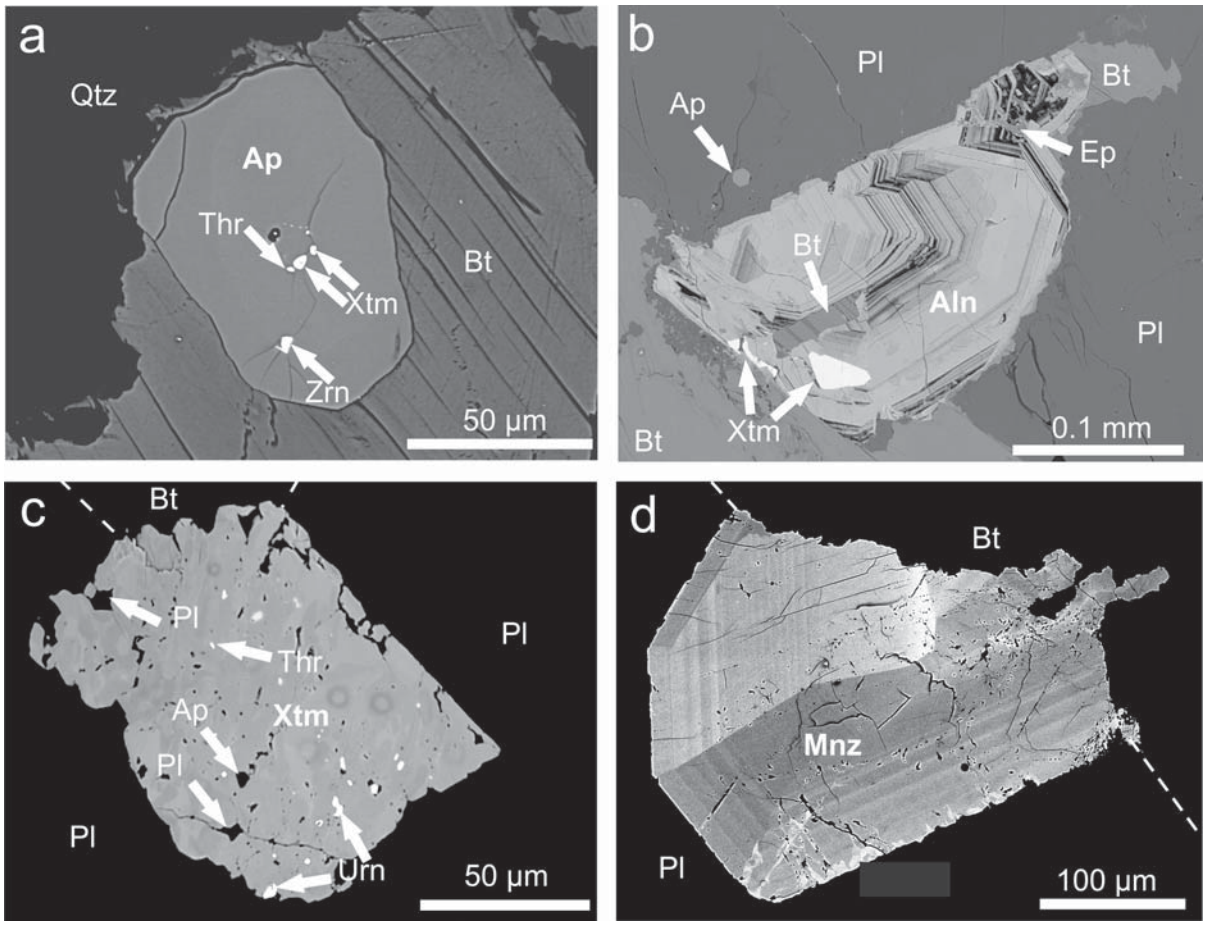

Text-fig. 4. BSE images of primary (magmatic) accessory phases. **a** – Fluorapatite included in biotite in granodiorite contains small inclusions of zircon, $ThSiO_4$ and xenotime. **b** – Oscillatory zoned allanite in the biotite granodiorite. Bright inclusions are xenotime. **c** – Xenotime with uraninite and $ThSiO_4$ inclusions, at biotite-plagioclase contact in enclave. **d** – Large, originally euhedral monazite-(Ce), showing a combination of sector and oscillatory zoning and with one edge heavily resorbed. At plagioclase-biotite contact in enclave. Abbreviations: aln – allanite; thr – $ThSiO_4$, urn – uraninite; xtm – xenotime; zrn – zircon

phic crystals up to 0.5 mm, many showing oscillatory zoning (Text-fig. 4b). Primary xenotime is rare, occurring as inclusions in allanite (Text-fig. 4b).

Detailed petrographical descriptions were given by Majerowicz (1963, 1972).

Microgranular magmatic enclaves

The microgranular magmatic enclaves *sensu* Barbarin (1988) in the biotite granodiorite occur as discrete individual bodies or in swarms. Their occurrence is not associated with proximity to the margins of the intrusion. They range in size from 3 to 50 cm but are mostly 5–15 cm in diameter. Their shape is oval or sub-spherical, they are finer-grained than the host rocks, occasionally porphyritic, and contain higher amounts of mafic minerals. Smaller enclaves tend to be darker than larger ones. In the Strzeblów quarry the enclaves constitute no more than a few percent of the body. They are rather uniformly distributed in the host but sometimes form several narrow vertical trains, or swarms (Text-fig. 2a). The contact between enclave and host rock changes from sharp, but unchilled, to diffuse over a distance of a few centimetres. Felsic areas have sometimes formed on the granodiorite side of the contact, seen as a light "halo" round the enclaves (Text-fig. 2a). Locally enclaves are mantled by biotite crystals (Text-fig. 2b), probably due to the adherence of mafic minerals to the border of the enclave by surface tension (Barbarin and Didier 1991).

The enclaves are fine-grained, with crystals, 0.1–0.5 mm in size, of plagioclase (50–62%), biotite

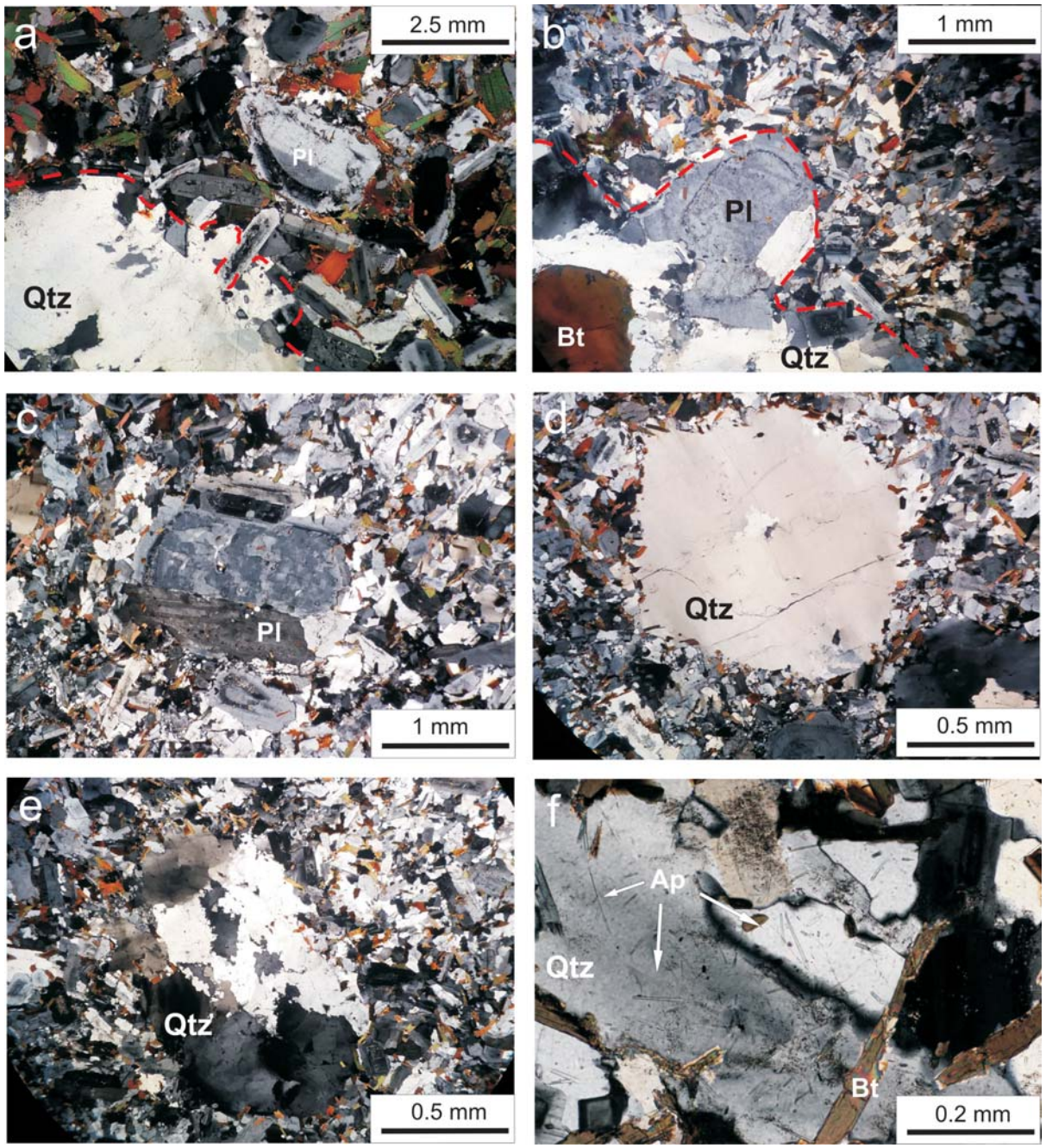

Text-fig. 5. Photomicrographs of the biotite granodiorite and mafic magmatic enclaves. **a** – The boundary between the biotite granodiorite and enclave; lath-shaped plagioclase projecting from the margins of enclave outwards and growth in quartz; inside the enclave is a visible large plagioclase xenocryst. **b** – Plagioclase from the biotite granodiorite crosses the border with enclave. **c** – Plagioclase xenocryst with boxy cellular texture (core) and anorthite spikes (rim) in enclave. **d** – Ocellar quartz mantled by biotite in enclave. **e** – Quartz aggregates in enclave. **f** – Acicular apatites in enclave. Abbreviations: ap – apatite; bt – biotite; pl – plagioclase; qtz – quartz

(30–35%), quartz (5–18%) and K-feldspar (0–5%). Accessory phases are apatite, monazite, zircon, allanite, xenotime and opaque minerals. Euhedral laths of plagioclase occur mostly as a groundmass phase. It shows distinct normal, reverse and/or oscillatory zoning (An_{37} to An_9) (Text-fig. 3c).

Sometimes laths of crystals can also be observed projecting from the margins of the enclave outwards

and growth in K-feldspar or quartz (Text-fig. 5a). Large euhedral or subhedral, normal or patchily zoned (Text-fig. 3c), crystals up to 5 mm are sometimes present on the border of (Text-fig. 5b) or inside an enclave (Text-figs 2b, 3c, 5c). It is generally rounded by resorption, and often shows a anorthite-rich spike zone in the rim (Text-fig. 5 a, c). The cores of plagioclase xenocrysts are less calcic, with An contents reaching 38%, similar to the granodioritic plagioclases (Text-fig. 3c).

Biotite occurs as elongated, lath-shaped grains or as inclusions in plagioclase. It forms from anhedral to euhedral flakes, containing inclusions of zircon, apatite, allanite, monazite and xenotime. It is compositionally very similar to biotite in the granodiorite, with $^{IV}Al = 2.9–3.0$ apfu and 100.Fe*/(Fe*+Mg) ratios of ~64.

Anhedral quartz is a late-crystallizing phase and fills the interstices between plagioclase and biotite or forms poikilitic grains. Rare biotite-rimmed quartz ocelli and oval to ellipsoidal quartz aggregates a few mm in size are observed in some enclaves (Text-fig. 5d, e)

K-feldspar (0–5%) is usually rare and if present, forms interstitial grains between plagioclase and biotite or enclosing them, suggesting a late growth phase.

Apatite is the main accessory mineral, forming needles up to 0.5 mm (but most often <0.1 mm), usually enclosed in plagioclase (Text-fig. 5f). A zone particularly rich in acicular apatite extends for 1–2 mm into the enclaves.

Monazite is the dominant accessory phase located on the boundary between host granodiorite and tonalitic enclaves (Text-figs 4d, 6). Most are located within the rim zone of enclaves and show the clear oscillatory zoning typical of a magmatic origin. Compositional zoning is most prominent in the Th content (in some large crystals varying from 23.8% in the core to 2% Th in the rim). As in the granodiorite, primary xenotime is rare. The originally magmatic crystal shown in Text-fig. 3c contains rounded uraninite and $ThSiO_4$ inclusions.

The host biotite granodiorite-enclave contact zone

The contact zones between granodiorite and enclaves are diverse on the scale of a few centimeters (Text-fig. 2b). Compared to the normal granodiorite, they are poor in mafic minerals, forming a felsic halo around the enclaves (cf. Text-fig. 2b). These zones are considered to result from the chemical exchange between mafic and felsic melt (Barbarin and Didier 1991). The plagioclase has commonly been rendered turbid by hydrothermal fluids, which have also caused partial chloritization of the biotite. It appears that the contact zone was a preferential pathway for fluid movement. The contact area is also heavily cracked, with the partial development of a crudely mosaic texture, the texture possibly being due to late-stage differential movement between more mafic magma blobs and the partially crystallized granitic host.

As noted above, monazite is the dominant accessory phase in the contacts between granodiorite and the studied enclaves (Text-fig. 6). The largest crystals occur close to the boundaries of the lithologies, particularly where enclaves occur a few cm apart. It occurs as inclusions in biotite and plagioclase, implying that it started to grow early in the crystallization sequence, or is interstitial, forming euhedral to subhedral grains. The long dimensions of the crystals vary from tens of μm up to 500 μm (Text-fig. 3d). Wolf and London (1995) considered monazite >100 μm as "large" and Förster (1998) considered the size of "normal" monazite-(Ce) to be in the range 20 μm to >200 μm. Townsend *et al.* (2000) reported crystals ≥200 microns in the Ireteba granite, Southern Nevada, and Broska *et al.* (2000) found monazites of 300–500 μm size in granitoids of the Tribeč Mountains, Western Carpathians. Lisowiec *et al.* (2013) recorded monazite up to 300 μm in size in the Stolpen granite, Germany. The Strzegom crystals are, therefore, relatively large for magmatic monazites. In a thin section, the number of monazite crystals larger than ~20 μm within the granodiorite-enclave contact zone can exceed 50, whilst within the granodiorite the number is usually below ten.

The magmatic monazite is almost invariably zoned, the zoning textures being divisible into three types, rather similar to those recognized by Townsend *et al.* (2000) in monazite from the Ireteba granite, southern Nevada. (i) Euhedral, commonly showing oscillatory zoning (m1, m4, m6). (ii) Sector zoning, comprising angular areas of different brightness on back-scattered electron (BSE) images, sometimes associated with oscillatory zoning (Text-fig. 3d). (iii) A notable feature, especially of variants of types 1 and 2, is strong marginal resorption, often restricted to one edge (Text-fig. 3d). In some grains, the oscillatory zoning is disturbed by patchy zones and veins.

WHOLE-ROCK GEOCHEMISTRY

The biotite granodiorites and enclaves are mildly peraluminous, with alumina saturation indices (ASI; molecular $Al_2O_3/(CaO+Na_2O+K_2O)$) close to 1.05 and

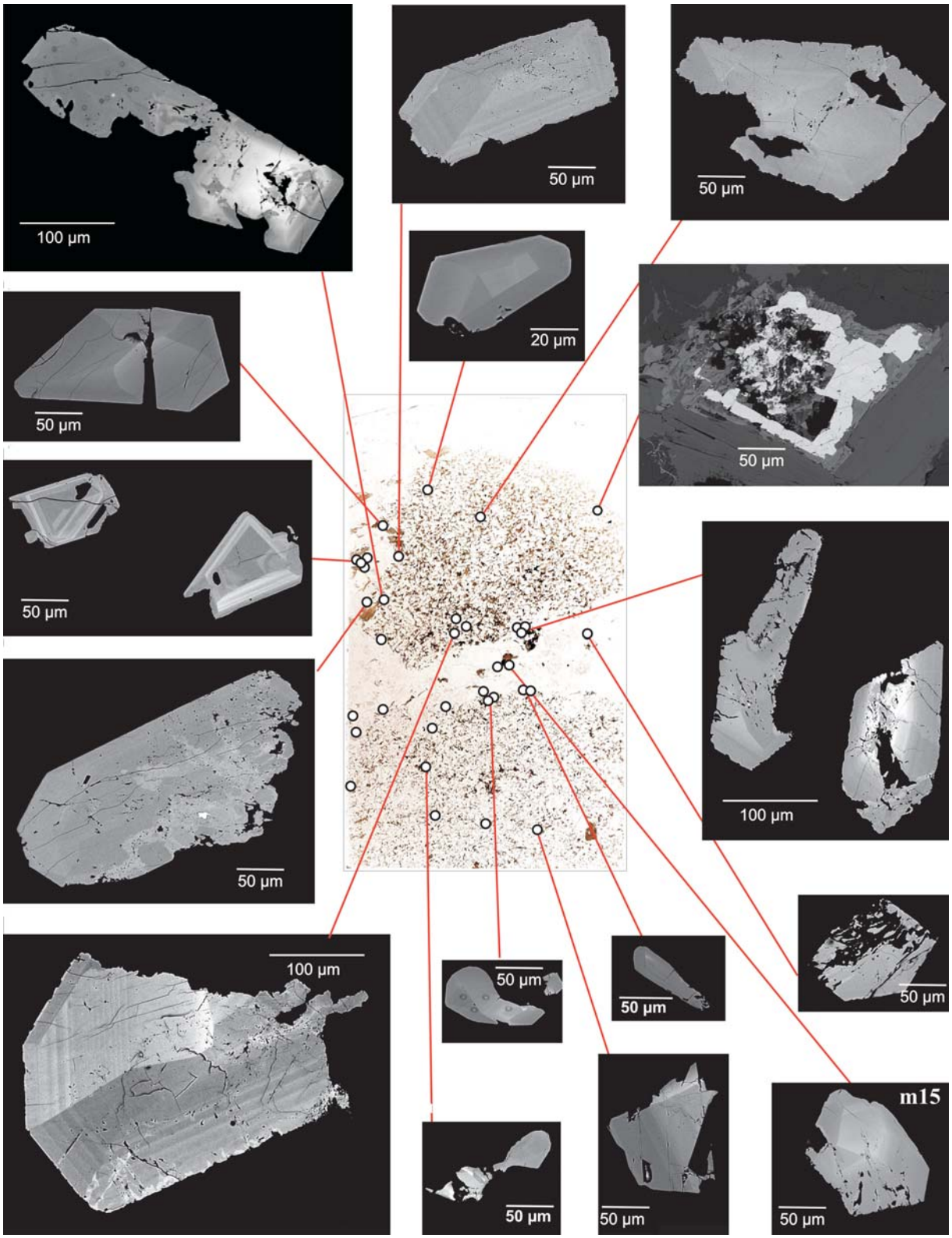

Text-fig. 6. Photomicrograph of contact zone between the biotite granodiorite and enclave. Note the large amount of monazite-(Ce) crystals with different morphology

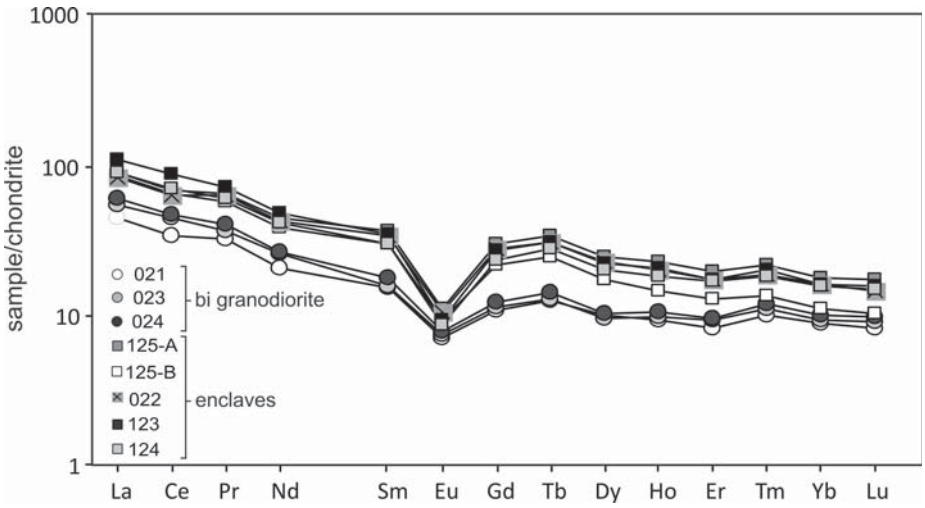

Text-fig. 7. Chondrite-normalised REE patterns for selected biotite granodiorites and enclaves. Normalizing factors from Sun and McDonough (1989)

ranging from 1.04 to 1.10, respectively (Table 1 and our unpublished data). According to the geochemical classification of Frost *et al.* (2001), the rocks are mainly magnesian and intermediate between calc-alkaline and alkali-calcic. The SiO_2 content of the granodiorites ranges from 72.6 to 74.1 wt.%, whilst the enclaves contain from 62.1 to 68.2 wt.% SiO_2. The enclaves have higher contents of Al_2O_3, TiO_2, total Fe as Fe_2O_3, MnO, MgO, CaO, P_2O_5, Co, V, Na_2O, Cs, Rb, Ga, Zr, Hf, Nb, Ta, REE and Y, and lower contents of K_2O and Ba. Chondrite-normalised REE patterns of the host granodiorite are similar and subparallel to those of the enclaves (Text-fig. 7). The enclaves generally have higher contents of all REE, higher La_N/Yb_N (for granodiorites from 5.1 to 5.9 and for enclaves between 5.0 and 7.7; Table 1) and similar to, or larger negative Eu anomalies than, the host rocks (for granodiorite Eu/Eu* = 0.52–0.56, for enclaves: 0.30–0.36).

DISCUSSION

Textural evidence for magma mingling

The presence of microgranular, dark enclaves in a felsic host is considered important evidence of interaction of contrasting in composition melts. Magmas of different compositions, different temperatures, and different stages of crystallization can mix and/or mingle with each other. The term "mixing" is used to describe hybrid rocks whose original components have been obscured. The term "mingling" refers to the interaction of contrasting magmas whose composition has been changed to some extent but which have partly retained their original features. Dark microgranular enclaves are produced by mingling between mafic and felsic magmas. The different types of interaction between coexisting magmas may indicate that hybridisation processes occur at different stages in the evolution of the magma system. Although mafic magmatic enclaves have been identified in many granitic bodies, their origin is still debated. Several models have been proposed for their origin. The common interpretation implies that enclaves represent mafic magma "blobs" (Zorpi *et al.* 1989) or "globules" (Vernon 1984), probably produced from the mantle, that have mingled or partly mixed with felsic magmas derived from the crust (Didier 1973; Reid *et al.* 1983; Vernon 1984, 1991, 2000; Barbarin and Didier 1991; Castro *et al.* 1990; Barbarin and Didier 1991; Orsini *et al.* 1991; Poli and Tommasini 1991; Elburg 1996; Collins *et al.* 2000; Słaby and Martin 2008; Słaby *et al.* 2008; Perugini and Poli 2012; Chen *et al.* 2015). Another model assumes a restitic origin for the enclaves (Chappell *et al.* 1987; Chen *et al.* 1990; Chappell and White 1991; White *et al.* 1999). That model interprets the enclaves as representing the solid residues of refractory minerals from the partial melting of the source rocks of the granitoid. A model suggesting that enclaves represent disrupted cumulates or the fine-grained, chilled margin of the magma chamber was proposed by Fershtater and Borodina (1977, 1991), Phillips *et al.* (1981), Dodge and Kistler

Sample	021	023	024	022	123	124	125-A	125-B
type	granite	granite	granite	enclave	enclave	enclave	enclave	enclave
wt %								
SiO_2	74.08	72.57	73.07	62.76	64.70	65.55	63.06	67.16
TiO_2	0.19	0.25	0.27	0.87	0.72	0.69	0.82	0.59
Al_2O_3	13.97	14.47	14.56	17.48	16.55	16.21	17.10	16.39
Fe_2O_3 t	1.50	1.85	1.97	5.68	4.88	4.76	5.61	3.97
MnO	0.04	0.06	0.07	0.16	0.15	0.15	0.16	0.12
MgO	0.37	0.49	0.53	1.68	1.38	1.34	1.64	1.13
CaO	1.59	1.89	1.83	3.61	2.97	2.97	3.35	2.96
Na_2O	3.78	4.16	4.14	4.64	5.05	4.80	4.79	5.25
K_2O	3.87	3.42	3.51	2.13	1.93	1.84	2.11	1.57
P_2O_5	0.08	0.06	0.06	0.38	0.28	0.24	0.36	0.23
LOI	0.30	0.20	0.25	0.40	0.30	0.60	0.80	0.60
Total	99.82	99.55	100.40	99.80	99.42	99.59	99.80	99.97
A/CNK	1.05	1.03	1.04	1.06	1.05	1.06	1.05	1.04
Mg no.	0.33	0.34	0.35	0.37	0.36	0.36	0.37	0.36
ppm								
Ba	584	590	547	507	332	360	463	352
Cs	4	4	6	9	10	10	11	7
Rb	110	115	138	143	157	150	165	119
Sr	230	268	263	355	256	297	355	288
V	13	15	16	55	42	43	58	37
Co	4	3	3	7	6	6	8	5
Zr	84	100	111	155	210	181	170	173
Hf	3	3	4	5	6	6	5	5
Y	19	22	23	43	45	42	47	30
Nb	10	14	17	27	35	36	31	26
Ta	1	1	3	2	3	3	2	2
U	6	5	5	9	4	4	18	4
Th	10	11	11	5	8	9	5	8
La	13.9	17.1	18.5	26.1	34.4	27.7	27.6	26.6
Ce	27.6	36.0	38.0	52.3	71.3	56.4	55.2	53.1
Pr	3.4	3.9	4.25	6.61	7.62	6.4	6.81	6.11
Nd	12.2	15.4	15.7	25.4	28.7	24.4	26.6	22.9
Sm	2.9	3.0	3.4	6.5	6.6	5.7	7.0	5.8
Eu	0.5	0.5	0.6	0.8	0.7	0.6	0.81	0.7
Gd	2.8	2.9	3.2	7.2	7.0	6.1	7.8	5.7
Tb	0.6	0.6	0.6	1.4	1.4	1.2	1.5	1.1
Dy	3.2	3.0	3.3	7.4	7.2	6.4	8.0	5.5
Ho	0.6	0.6	0.7	1.3	1.3	1.2	1.5	1.0
Er	1.7	2.0	2.0	3.6	3.7	3.6	4.1	2.7
Tm	0.3	0.3	0.3	0.5	0.6	0.5	0.6	0.4
Yb	1.8	1.9	2.1	3.3	3.3	3.2	3.7	2.3
Lu	0.3	0.3	0.3	0.5	0.5	0.5	0.5	0.3
$(La/Yb)_N$	5.14	5.86	5.89	5.24	6.97	5.70	4.97	7.67
Eu/Eu*	0.55	0.56	0.52	0.34	0.30	0.33	0.34	0.36

Table 1. Representative composition of biotite granodiorite and enclaves. LOI – loss of ignition; A/CNK = $Al_2O_3/(CaO+NaO+K_2O)$ molar; Mg no. = atomic $Mg/(Mg+Fe^{2+})$; Eu/Eu* = $[EuN/\sqrt{(Sm_N*Gd_N)}]$; N – chondrite normalized to values of Nakamura 1974

(1990), Flood and Shaw (2014), Dorais *et al.* (1997) Dahlquist (2002), Chen W.S. *et al.* (2007), Chen S. *et al.* (2015) or Lee *et al.* (2015). A xenolithic origin for the dark enclaves was suggested by Elburg (1996) and Clemens and Elburg (2013).

However, we present here textures that point to the interaction between the melts of contrasting composition and not to the origin of the enclaves. The internal textures of the enclaves from the eastern part of the Strzegom-Sobótka massif are described for the first time. The spherical to ellipsoidal shapes, fine-grained chilled margins, felsic haloes, and scarce zoned enclaves with discontinuous hybrid zones at enclave-host contacts may suggest they are quenched blobs of silica-poor magma that intruded the granitic host (Didier and Barbarin 1991; Barbarin and Didier 1992; Wiebe and Collins 1998). The presence of such textures indicates that the mafic or hybridic, with intermediate composition magma was probably injected into the magma chamber at the final emplacement level (Barbarin and Didier 1992) and was scattered throughout the pluton by convection. The fine grain size of the enclaves is consistent with rapid crystallization due to thermal equilibration between the high-temperature, probably low-viscosity magma and relatively low-temperature, high-viscosity granitic magma (Vernon 1984; Fernandez and Barbarin 1991).

The local concentration of enclaves into polygenic swarms may have been caused by segregation (Barbarin and Didier 1992; Collins *et al.* 2000). The appearance of polygenic swarms of enclaves may indicate the proximity to the marginal part of the magma chamber of the channels with which the more mafic magma was injected into almost solidified granodiorite (Janoušek *et al.* 2000; Barbarin 2005).

According to Hibbard (1991), no single texture can be used to prove the occurrence of magma mixing-mingling processes. We have described the combination of textures pointing to these interactions, such as plagioclase with disequilibrium textures from the host biotite granodiorite-enclave contact zone (Text-fig. 3b), plagioclase xenocrysts with disequilibrium textures inside the enclaves (Text-fig. 3d), small plagioclase laths and blade-shape biotite building up a framework in the enclave matrix (Text-fig. 5a–e), quartz ocelli (Text-fig. 5d), ellipsoid quartz aggregates (Text-fig. 5e) and the acicular morphology of apatite (Text-fig. 5f).

Megacrysts of plagioclase with disequilibrium textures occur in both the host granodiorite and enclaves. These crystals display patchily zoned cores (i.e. boxy cellular texture) and combinations of several continuous/discontinuous oscillatory zones in the rim. The more calcic, anorthite-rich, zone in less calcic plagioclase crystals was described by Wiebe (1968) as an anorthite 'spike' and linked with magma mixing. Between the inner and outer parts of crystals resorption zones are observed (Text-figs 3d, 5c). The resorption-regrowth textures may be connected with local superheating of felsic magma by contact with injected mafic magma blobs and reflect rapid changes in magma composition (Hibbard 1991). After dissolution, they have re-grown in more primitive magma by regaining the equilibrium at the crystal-melt interface (Tsuchiyama 1985).

The presence of porphyrocrysts of plagioclase inside enclaves can be interpreted as their having moved from the granitic into mafic melts (Barbarin and Didier 1991; Hibbard 1991; Waight *et al.* 2000) and therefore they will be referred as xenocrysts. The process has been documented from many plutons in the Sudetes: Janoušek *et al.* (2004), for example, reported that partly grown plagioclase crystals were exchanged, sometimes repetitively, during mixing of basic and acidic magmas in the Sávaza intrusion, Czech Republic, and Słaby and Götze (2004) and Słaby *et al.* (2007) recorded megacryst movement between melts in the Karkonosze pluton in the Western Sudetes; Pietranik and Koepke (2014) documented plagioclase transfer in dioritic and granodioritic rocks from the Gęsiniec Intrusion (Strzelin Massif). Such textures have also been described from the western part of the Strzegom massif (Domańska-Siuda and Słaby 2005; Domańska-Siuda 2007; Domańska-Siuda *et al.* 2019).

The fine-grained enclave matrix is composed mainly of small lath-shaped plagioclases (Text-fig. 5a–e). Most display normal zoning, with core compositions related to an early stage of crystallization from more mafic magma and rims reflecting equilibration with the new, hybrid melt (Hibbard 1991). Their elongate habit results from relatively rapid crystallization, favoured by a high nucleation rate.

Biotite-rimmed quartz ocelli may also be explained as a result of magma interactions (Hibbard 1991). Quartz crystals were introduced from a felsic to a more mafic, unstable system. Marginal dissolution of quartz extracts heat of crystallization from the adjacent melt, causing local under-cooling and promoting nucleation of mafic minerals (Baxter and Feely 2002).

The acicular morphology of apatite is different to that in granodiorite and reflects growth under conditions of relatively fast quenching of the mafic magma (Wyllie *et al.* 1962; Hibbard 1991). The abundance of acicular apatite, especially in the outer parts of the

enclaves, can support this process. Another texture linking with magma mixing-mingling is the presence of mixed apatite morphologies, where acicular apatites coexist with prismatic forms (Hibbard 1991). Prismatic apatite occurs in granodiorite in close proximity to enclave (Text-fig. 4a), in the zone undoubtedly changed by the interacting melts.

The presence of large monazite-(Ce) crystals close to the boundaries between granodiorite and dark, microgranular enclaves is an uncommon feature in the intrusion, occurring only where enclaves are closely packed, within a few cms of each other (Text-figs 2, 6). This may suggest that their formation is also linked to temperatures locally elevated due to the presence of the hotter, more mafic and enriched in REE melt. This promoted crystal growth by lowering melt viscosity and promoting faster diffusion of elements to crystal faces (Orsini *et al.* 1991; Wark and Miller 1993). It was noted above that the granodiorite zones between enclaves commonly show hydrothermal alteration of the main minerals and cataclastic texture. Hence, fluid ingress and deformation may also have promoted crystal growth. Further evidence of the growth mechanism may come from oscillatory zoning.

Oscillatory zoning in monazite-group minerals (Text-fig. 6) is usually ascribed to crystallization under magmatic conditions (Broska *et al.* 2000; Townsend *et al.* 2000; Dini *et al.* 2004). This type of zoning can, in general, be ascribed to two mechanisms (Bottinga *et al.* 1966): (i) repeated changes in the T, P, pH_2O and melt composition as conditions within or external to the magma reservoir change, or when there is relative movement between melt and crystals; and (ii) the kinetics of the processes acting at the crystal-melt interface. Both mechanisms may have acted during growth of the monazites in the hybrid magma.

Even when the enclaves had reached the point of critical crystallinity (Marsh 1996) and showed no internal movement of crystals and residual melt, they would still have been plastic. They would also have been enclosed in granodiorite magma which was still relatively mobile. Due to the differing viscosities and densities of the two lithologies, the margins of the enclaves would have 'seen' melts of different bulk composition and perhaps pH_2O. The compositional differences between the lighter and darker zones thus reflected the contact of the growing crystals with melts of varying LREE and Si content (Orsini *et al.* 1991).

Alternatively, the oscillatory zoning was dependent on the kinetics of processes acting at the interface between the melt and the growing crystal faces. Where the rate of crystal growth was not balanced by rates of element diffusion, chemical boundary layers, enriched and then depleted in LREE and Si may have developed, represented by the zones in the crystals. The large size and abundance of monazite seem to argue, however, for relatively rapid crystal growth which was facilitated by contact with new, more mafic, enriched in REE melt.

The strong marginal resorption shown by some grains (Text-fig. 6) can also be ascribed to their being brought into contact with melts of different composition and/or temperature.

The stability of monazite in silicate melts depends on numerous compositional parameters of the melt, such as the activities of SiO_2, CaO and P_2O_5, the oxygen fugacity, the peraluminosity, and the ratios and contents of the lanthanides and actinides (Förster 1998). The stability relationships between monazite, allanite and apatite are controlled mainly by the Ca activity and melt peraluminosity (Wolf and London 1995; Broska *et al.* 2000; Seydoux-Guillaume *et al.* 2002; Dini *et al.* 2004). Budzyń *et al.* (2011), for example, have shown that in the presence of F, high Ca activity destabilizes monazite and promotes the formation of fluorapatite and REE-epidote or allanite. Given that the monazite in the granodiorite has low CaO contents (0.37–0.81 wt.%), the inferred high Ca activity must have been provided by the fluids.

Chemical dating of monazite-(Ce)

Monazite grains were dated with the EMP Cameca SX-100 microprobe (details are given in the Analytical methods section), using the Cameca programme for chemical dating. 106 points were analyzed. The most extreme 19 results were rejected, leaving 87 point analyses (Text-fig. 8). Statistical calculations were executed using Isoplot 3 (Ludwig 1991). The final result of 297 ± 11 Ma is in good agreement with the zircon ages presented by Turniak *et al.* (2014) and monazite (Turniak *et al.* 2011).

CONCLUSIONS

Petrological observations in the biotite granodiorite and enclaves with tonalitic composition lead to the following conclusions:

- the enclaves are igneous in origin and comprise plagioclase, biotite, and small amount quartz with accessory apatite, monazite and zircon;

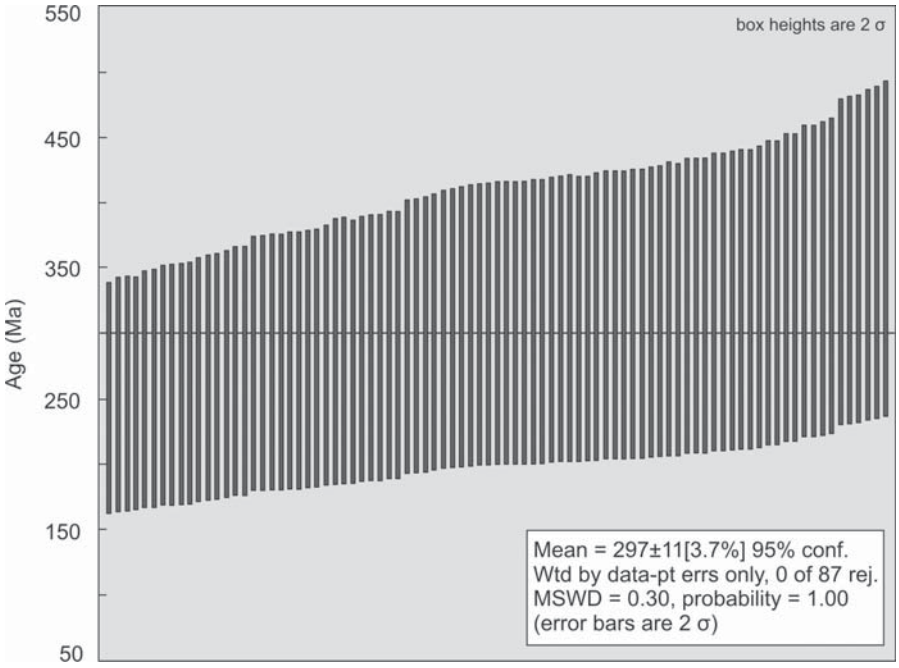

Text-fig. 8. Monazite weighted average ages of 87 point analyses

- the enclaves show petrographic features that are compatible with magma mixing-mingling. The textures include numerous acicular apatite microcrystals, plagioclase xenocrysts incorporated into the enclaves showing distinct reversed and/or oscillatory zoning with resorption surfaces, plagioclase with anorthite spike zoning, biotite-rimmed ocellar quartz, ellipsoid quartz aggregates;
- we also relate the unusual growth of numerous monazite crystals to the process of magma mixing-mingling. Crystallization of monazite might be linked to the higher temperatures locally elevated due to the presence of the hotter, more mafic and enriched in REE melt. This probably promoted crystal growth by lowering melt viscosity and increasing the rate of diffusion of elements to crystal faces. A change of temperature and/or composition of the melt could be also responsible for resorption of many smaller monazite crystals.

Petrographic observations demonstrate that the microgranular magmatic enclaves represent globules of hybrid magma formed as a result of mingling with more felsic host melt. The local concentration of enclaves into polygenic swarms may by caused by segregation processes and their appearance may indicate proximity to the marginal part of the magma chamber.

Acknowledgments

We thank Ray Macdonald and Ewa Słaby for very helpful comments on the manuscript. We are very grateful to Ms Lidia Jeżak for assistance in the microprobe laboratory. Funding for the project was supplied by IGMiP BSt 173504/39/2015.

REFERENCES

Awdankiewicz, M., Awdankiewicz, H., Rapprich, V. and Starkova, M. 2014. A Permian andesitic tuff ring at Rožmital (the Intra-Sudetic Basin, Czech Republic) – evolution from explosive to effusive and highlevel intrusive activity. *Geological Quarterly*, **58** (4), 759–778.

Bacon, C.R. 1986. Magmatic inclusions in silicic and intermediate volcanic rocks. *Journal of Geophysical Research, Solid Earth*, **91** (B6), 6091–6112.

Bacon, C.R. and Druitt, T.H. 1988. Compositional evolution of the zoned calcalkaline magma chamber of Mount Mazama, Crater Lake, Oregon. *Contribution to Mineralogy and Petrology*, **98**, 224–256.

Barbarin, B. 1988. Field evidence for successive mixing and mingling between the Piolard Diorite and the Saint-Julien-la-Vêtre Monzogranite (Nord-Forez, Massif Central, France). *Canadian Journal of Earth Sciences*, **25**, 49–59.

Barbarin, B. 2005. Mafic magmatic enclaves and mafic rocks associated with some granitoids of the central Sierra Neva-

da batholith, California: nature, origin, and relations with the hosts. *Lithos*, **80**, 155–177.

Barbarin, B. and Didier, J. 1991. Microscopic features of mafic microgranular enclaves. In: Didier, J. and Barbarin, B. (Eds), Enclaves and granite petrology, pp. 253–262. Elsevier; Amsterdam.

Barbarin, B. and Didier, J. 1992. Genesis and evolution of mafic microgranular enclaves through various types of interaction between coexisting felsic and mafic magmas. *Transactions of the Royal Society of Edinburgh: Earth Sciences*, **83**, 145–153.

Baxter, S. and Feely, M. 2002. Magma mixing and mingling textures in granitoids: examples from the Galway Granite, Connemara, Ireland. *Mineralogy and Petrology*, **76**, 63–74.

Birski, Ł., Słaby, E. and Domańska-Siuda, J. 2018. Origin and evolution of volatiles in the Central Europe late Variscan granitoids, using the example of the Strzegom-Sobótka Massif, SW Poland. *Mineralogy and Petrology*, DOI: 10.1007/s00710-018-0615-6

Bottinga, Y., Kudo, A. and Weill, D. 1966. Some observations on oscillatory zoning and crystallization of magmatic plagioclase. *American Mineralogist*, **51**, 792–806.

Broska, I., Petrík, I. and Williams, C.T. 2000. Coexisting monazite and allanite in peraluminous granitoids of the Tribeč Mountains, Western Carpathians. *American Mineralogist*, **85**, 22–32.

Bruckener, H.K., Blusztajn, J. and Bakun-Czubarow, N. 1996. Trace element and Sm-Nd 'age' zoning in garnets from peridotites of the Caledonian and Variscan mountains and tectonic implications. *Journal of Metamorphic Geology*, **14**, 61–73.

Budzyń, B., Harlov, D.E., Williams, M.L. and Jercinovic, M.J. 2011. Experimental determination of stability relations between monazite, fluorapatite, allanite, and REE-epidote as a function of pressure, temperature, and fluid composition. *American Mineralogist*, **96**, 1547–1567.

Castro, A., Moreno-Ventas, I. and de la Rosa, J.D. 1990. Microgranular enclaves as indicators of hybridization processes in granitoid rocks, Hercynian Belt, Spain. *Geological Journal*, **25**, 391–404.

Chappell, B.W. and White, A.J.R. 1991. Restite enclaves and the restite model. In: Didier, J., and Barbarin, B. (Eds), Enclaves and Granite Petrology, pp. 375–381. Elsevier; Amsterdam.

Chappell, B.W., White, A.J.R. and Wybom, D. 1987. The importance of residual source material (restite) in granite petrogenesis. *Journal of Petrology*, **28**, 1111–1138.

Chen, S., Niu, Y., Sun, W., Zhang, Y., Li, J., Guo, P. and Sun, P. 2015. On the origin of mafic magmatic enclaves (MMEs) in syn-collisional granitoids: Evidence from the Baojishan pluton in the North Qilian orogen, China. *Mineralogy and Petrology*, **109**, 577–596.

Chen, W.F., Chen, P.R., Huang, H.Y., Ding, X. and Sun, T. 2007. Chronological and geochemical studies of granite and enclave in Baimashan pluton, Hunan, South China: Science in China. *Series D, Earth Sciences*, **50**, 1606–1627.

Chen, Y.D., Price, R.C., White, A.J.R. and Chappell, B.W. 1990. Mafic inclusions from the Glenbog and Blue Gum Granite Suites, southeastern Australia. *Journal of Geophysical Research*, **95**, 17,757–17,785.

Clemens, J.D. and Elburg, M.A. 2013. Comment – Origin of enclaves in S-type granites of the Lachlan Fold Belt. *Lithos*, **175–176**, 351–352.

Collins, W.J., Richards, S.R., Healy, B.E. and Ellison, P.I. 2000. Origin of heterogeneous mafic enclaves by two-stage hybridisation in magma conduits (dykes) below and in granitic magma chambers. Transactions of the Royal Society of Edinburgh. *Earth Sciences*, **91**, 27–45.

Dahlquist, J.A. 2002. Mafic microgranular enclaves: Early segregation from metaluminous magma (Sierra de Chepes), Pampean Ranges, NW Argentina. *Journal of South American Earth Sciences*, **15**, 643–655.

Didier, J. 1973. Granites and their enclaves; the bearing of enclaves on the origin of granites, 393 p. Elsevier Scientific Pub. Co.; Amsterdam, London & New York.

Didier, J. and Barbarin B. 1991. The different types of enclaves in granites-Nomenclature. In: Didier, J. and Barbarin, B. (Eds), Enclaves and granite petrology, pp. 19–23. Elsevier; Amsterdam.

Dini, A., Rocchi, S. and Westerman, D.S. 2004. Reaction microtextures of REE-Y-Th-U accessory minerals in the Monte Capanne pluton, Elba Island, Italy): a possible indicator of hybridization processes. *Lithos*, **78**, 101–118.

Dodge, F.D.W. and Kistler, R.W. 1990. Some additional observations on inclusions in the granitic rocks of the Sierra Nevada. *Journal of Geophysical Research Atmospheres*, **95**, 17841–17848.

Domańska-Siuda, J. 2007. The granitoid Variscan Strzegom-Sobótka massif. In: Kozłowski, A. and Wiszniewska, J. (Eds), Granitoids in Poland. *Archivum Mineralogiae Monograph*, **1**, 179–191.

Domańska, J. and Słaby, E. 2004. The hornblende-biotite-granite from Strzegom-Sobótka massif – parental magma evolution. *Mineralogical Society of Poland, Special Papers*, **24**, 131–134.

Domańska-Siuda, J. and Słaby, E. 2005. One-sided contamination of lamprophyric melt drops in hornblende-biotite granite magma chamber – a case study of Strzegom massif (SW Poland). *Mineralogical Society of Poland, Special Papers*, **25**, 67–70.

Domańska-Siuda, J., Słaby, E. and Szuszkiewicz, A. 2019. Ambiguous isotopic and geochemical signatures resulting from limited melt interactions in a seemingly composite pluton: a case study from the Strzegom-Sobótka Massif (Sudetes, Poland). *International Journal of Earth Sciences.* DOI: 10.1007/s00531-019-01687-w

Dorais, M.J., Lira, R. and Chen, Y. 1997. Origin of biotite–apatite-rich enclaves, Achala Batholith, Argentina. *Contributions to Mineralogy and Petrology*, **130**, 31–46.

Dubińska, E., Bylina, P., Kozlowski, A., Dörr, W., Nejbert, K. and Schastok, J. 2004. U-Pb dating of serpentinization: Hydrothermal zircon from a metasomatic rodingite shell (Sudetic ophiolite, SW Poland). *Chemical Geology*, **203**, 183–203.

Elburg, M.A. 1996. Evidence of isotopic equilibration between microgranitoid enclaves and host granodiorite, Warburton granodiorite, Lachlan fold belt, Australia. *Lithos*, **38**, 1–22.

Femandez, A. and Barbarin, B. 1991. Relative rheology of coeval mafic and felsic magmas: nature of resulting interaction processes. Shape and mineral fabrics of maficc microgranular enclaves. In: Didier, J. and Barbarin, B. (Eds), Enclaves and granite petrology, pp. 116–128. Elsevier; Amsterdam.

Fershtater, G.B. and Borodina, N.S. 1977. Petrology of autoliths in granitic rocks. *International Geology Review*, **19**, 458–468.

Fershtater, G.B. and Borodina, N.S. 1991. Enclaves in the Hercynian granitoids of the Ural Mountains, USSR. In: Didier, J. and Barbarin, B. (Eds), Enclaves and granite petrology, pp. 83–94. Elsevier; Amsterdam.

Flood, R.H. and Shaw, S.E. 2014. Microgranitoid enclaves in the felsic Looanga monzogranite, New England Batholith, Australia: Pressure quench cumulates. *Lithos*, **198–199**, 92–102.

Förster, H.-J. 1998. The chemical composition of REE-Y-Th-U-rich accessory minerals in peraluminous granites of the Erzegebirge-Fichtelgebirge region, Germany, Part I: The monazite-(Ce)-brabantite solid solution series. *American Mineralogist*, **83**, 259–272.

Franke, W. 2000. The mid-European segment of the Variscides: tectonostratigraphic units, terrane boundaries and plate tectonic evolution. *Geological Society, London, Special Publications*, **179**, 35–61.

Frost, B.R., Barnes, C.G., Collins, W.J., Arculus, R.J., Ellis, D.J. and Frost, C.D. 2001. A geochemical classification for granitic rocks. *Journal of Petrology*, **42**, 2033–2048.

Gerdes, A. and Wörner, G. 2000. Hybrids, magma mixing and enriched mantle melts in post-collisional Variscan granitoids: the Rastenberg Pluton, Austria. *Geological Society, London, Special Publications*, **179**, 415–431.

Henk, A. 1997. Gravitational orogenic collapse vs plate-boundary stresses: a numerical modelling approach to the Permo-Carboniferous evolution of Central Europe. *Geologische Rundschau*, **86**, 39–55.

Hibbard, M.J. 1991. Textural anatomy of twelve magma-mixed granitoid systems. In: Didier, J. and Barbarin, B. (Eds), Enclaves and granite petrology, pp. 431–444. Elsevier; Amsterdam.

Janoušek, V., Bowes, D.R., Braithwaite, C. and Rogers, G. 2000. Microstructural and mineralogical evidence for limited involvement of magma mixing in the petrogenesis of a Hercynian high-K calc-alkaline intrusion: the Kozárovice granodiorite, Central Bohemian Pluton, Czech Republic. *Transactions of the Royal Society of Edinburgh: Earth Sciences*, **91**, 15–26.

Janoušek, V., Braithwaite, C.J.R., Bowes, D.R. and Gerdes, A. 2004. Magma-mixing in the genesis of Hercynian calc-alkaline granitoids: an integrated petrographic and geochemical study of the Sávaza intrusion, Central Bohemian Pluton, Czech Republic. *Lithos*, **78**, 67–99.

Jokubauskas, P., Bagiński, B., Macdonald, R. and Krzemińska, E. 2018. Multiphase magmatic activity in the Variscan Kłodzko–Złoty Stok intrusion, Polish Sudetes: evidence from SHRIMP U–Pb zircon ages. *International Journal of Earth Sciences*, **107**, 1623–1639.

Kröner, A. and Hegner, E. 1998. Geochemistry, single zircon ages and Sm-Nd systematics of granitoids rocks from the Góry Sowie Block (Owl Mts), Polish West Sudetes: evidence for early Paleozoic arc-related plutonism. *Geological Society, London*, **155**, 711–724.

Kryza, R. and Awdankiewicz, M. 2012. Ambiguous geological position of Carboniferous rhyodacites in the Intra-Sudetic Basin (SW Poland) clarified by SHRIMP zircon ages. *Geological Quartely*, **56** (1), 55–66.

Kryza, R. and Fanning, M. 2004. The Góry Sowie granulites (Sudetes, SW Poland): preliminary results of SHRIMP U-Pb zircon geochronology. International workshop on petrogenesis of granulites and related rocks. Abstract Volume, pp. 45–46. Moravian Museum; Brno.

Kryza, R. and Pin, C. 2010. The Central-Sudetic ophiolites (SW Poland): petrogenetic issues, geochronology and palaeotectonic implications. *Gondwana Research*, **17**, 292–305.

Kural, S. and Morawski, T. 1968. Strzegom-Sobótka granitic massif. *Biuletyn Instytutu Geologicznego*, **227**, 33–74.

Laurent, A., Janousek, V., Magna, T., Schulmann, K. and Mikova, J. 2014. Petrogenesis and geochronology of a post-orogenic calc-alkaline magmatic association: the Zulova Pluton, Bohemian Massif. *Journal of Geosciences*, **59**, 415–440.

Lee, C.-T.A., Morton, D.M., Farner, M.J. and Moitra, P. 2015. Field and model constraints on silicic melt segregation by compaction/hindered settling: The role of water and its effect on latent heat release. *The American Mineralogist*, **100**, 1762–1777.

Lisowiec, K., Budzyń, B., Słaby, E., Renno, A.D. and Götze, J. 2013. Fluid-induced magmatic and post-magmatic zircon and monazite patterns in granitoid pluton and related rhyolitic bodies. *Chemie der Erde*, **73**, 163–179.

Lisowiec. K,, Słaby, E. and Förster, H.J. 2015. Polytopic Vector Analysis (PVA) modelling of whole-rock and apatite chemistry from the Karkonosze composite pluton (Poland, Czech Republic). *Lithos*, **230**, 105–120.

Ludwig, K.R. 1991. ISOPLOT, a plotting and regression program for radiogenic data. *USGS Open-file Report*, 91–445.

Maciejewski, S. and Morawski, T. 1975. Petrographic variability of granites from the Strzegom Massif. *Kwartalnik Geologiczny*, **19**, 47–65.

Majerowicz, A. 1963. Granit z okolic Sobótki i jego stosunek do osłony w świetle badań petrograficznych. *Archivum Mineralogiae*, **24**, 127–237.

Majerowicz, A. 1972. Strzegom-Sobótka granitoid massif. *Geologica Sudetica*, **6**, 7–96.

Marsh, B.D. 1996. Solidification fronts and magmatic evolution. *Mineralogical Magazine*, **60**, 5–40.

Mazur, S., Aleksandrowski, P., Turniak, K. and Awdankiewicz, M. 2007. Geology, tectonic evolution and Late Palaeozoic magmatism of Sudetes – an overview. In: Kozłowski, A. and Wiszniewska, J. (Eds), Granitoids in Poland. *Archivum Mineralogiae Monograph*, **1**, 59–87.

Michel, L., Wenzel, T. and Markl, G. 2016. Interaction between two contrasting magmas in the Albtal pluton (Schwarzwald, SW Germany): textural and mineral-chemical evidence. *International Journal of Earth Sciences*, **106**, 1505–1524.

Nakamura, N. 1974. Determination of REE, Ba, Fe, Mg, Na and K in carbonaceous and ordinary chondrites. *Geochimica Cosmochimica Acta*, **38** (5): 757–775.

Oberc-Dziedzic, T., Kryza, R., Pin, C. and Madej, S. 2013. Variscan granitoid plutonism in the Strzelin Massif (SW Poland): petrology and age of the composite Strzelin granite intrusion. *Geological Quarterly*, **57**, 269–288.

Olivier, G.J.H. Corfu, F. and Krough, T.E. 1993. U-Pb ages from SW Poland: evidence for a Caledonian suture zone between Baltica and Gondwana. *Journal of the Geological Society London*, **150**, 355–369.

Orsini, J.-B., Cocirta, C. and Zorpi, M.-J. 1991. Genesis of mafic microgranular enclaves through differentiation of basic magmas, mingling, and chemical exchange with their host granitoid magmas. In: Didier, J. and Barbarin, B. (Eds), Enclaves and granite petrology, pp. 445–465. Amsterdam; Elsevier.

Perugini, D. and Poli, G. 2012. The mixing of magmas in plutonic and volcanic environments: Analogies and differences. *Lithos*, **153**, 261–277.

Phillips, G.N., Wall, V.J. and Clemens, J.D. 1981. Petrology of the Strathbogie Batholith: A cordierite-bearing granite. *Canadian Mineralogist*, **19**, 47–63.

Pietranik, A. and Wright, T.E. 2008. Processes and sources during late Variscan diorite-tonalite magmatism: insights from plagioclase chemistry (Gęsiniec intrusion, NE Bohemian massif, Poland). *Journal of Petrology*, **49**, 1619–1645.

Pietranik, A. and Koepke, J. 2009. Interactions between dioritic and granodioritic magmas in mingling zones: plagioclase record of mixing, mingling and subsolidus interactions in the Gęsiniec Intrusion, NE Bohemian Massif, SW Poland. *Contributions to Mineralogy and Petrology*, **158**, 17–36.

Pietranik, A. and Koepke, J. 2014. Plagioclase transfer from a host granodiorite to mafic microgranular enclaves: diverse records of magma mixing. *Mineralalogy and Petrology*, **108**, 681–694.

Pin, C., Puziewicz, J. and Duthou, J.-L. 1988. Studium izotopowe Rb-Sr oraz Sm-Nd masywu granitowego Strzegom-Sobótka. In: Petrologia i geologia fundamentu waryscyjskiego polskiej części Sudetów, pp. 37–41. Wrocław.

Pin, C., Puziewicz, J. and Duthou, J.-L. 1989. Ages and origins of a composite granite massif in the Variscan belt: a Rb-Sr study of the Strzegom-Sobótka massif, W. Sudetes (Poland). *Neues Jahrbuch für Mineralogy (Abhandlungen)*, **160**, 71–82.

Poli, G.E. and Tommasini, S. 1991. Model for the origin and significance of microgranular enclaves in calc-alkaline granitoids. *Journal of Petrology*, **32**, 657–666.

Puziewicz, J. 1990, Masyw granitoidowy Strzegom-Sobótka. Aktualny stan badań. *Archivum Mineralogiae*, **45**, 135–152.

Reid, J.B., Evans, O.C. and Fates, D.G. 1983. Magma mixing in granitic rocks of the central Sierra Nevada, California. *Earth and Planetary Science Letters*, **66**, 243–261.

Scherrer, N., Engi, M., Gnos, E., Jacob, V. and Liechti, A. 2000. Monazite analysis: from sample preparation to microprobe age dating and REE quantification. *Schweizerische Mineralogische und Petrographische Mitteilungen*, **80**, 93–105.

Seydoux-Guillaume, A.-M., Paquette, J.-L., Wiedenbeck, M., Montel, J.-M. and Heinrich, W. 2002. Experimental resetting of the U-Th-Pb systems in monazite. *Chemical Geology*, **191**, 165–181.

Słaby, E. and Götze, J. 2004. Feldspar crystallization under magma-mixing conditions shown by cathodoluminescence and geochemical modelling – a case study from the Karkonosze pluton (SW Poland). *Mineralogical Magazine*, **68**, 561–577.

Słaby, E, Seltmann, R., Kober, B., Müller, A., Galbarczyk-Gasiorkowska, L. and Jefferies, T. 2007. LREE distribution patterns in zoned alkali feldspar megacrysts from the Karkonosze pluton, Bohemian Massif – implications for parental magma composition. *Mineralogical Magazine*, **71**, 155–178.

Słaby, E. and Martin, H. 2008. Mafic and felsic magma interaction in granites: the Hercynian Karkonosze Pluton (Sudetes, Bohemian Massif). *Journal of Petrology*, **49**, 353–391.

Słaby, E., Götze, J., Wörner G., Simon K., Wrzalik R. and Śmigielski M. 2008. K-feldspar phenocrysts in microgranular magmatic enclaves: a cathodoluminescence and geochemical study of crystal growth as a marker of magma mingling dynamics. *Lithos*, **105**, 85–97.

Sun, S.-S. and McDonough, W.F. 1989. Chemical and isotopic systematics of oceanic basalts: implications for mantle composition and processes. In: Saunders, A.D. and Norry, M.J. (Eds), Magmatism in the ocean basins. *Geological Society, London, Special Publications*, **42**, 313–345.

Szuszkiewicz, A. 2007. Secondary Ba-enriched domains in alkali feldspar phenocrysts from the monzogranites of the

western part of the Strzegom-Sobótka massif, SW Poland. *Mineralogia Polonica*, **31**, 279–282.

Tsuchiyama, A. 1985. Dissolution kinetics of plagioclase in the melt of the system diopside-albite-anorthite, and origin of dusty plagioclase in andesites. *Contributions to Mineralogy and Petrology*, **89**, 1–16.

Townsend, K.J., Miller, C.F, D'Andrea, J.L., Ayers, J.C., Harrison and T.M. and Coath, C.D. 2000. Low temperature replacement of monazite in the Ireteba granite, Southern Nevada: geochronological implications. *Chemical Geology*, **172**, 95–112.

Turniak, K., Tichomirowa, M. and Bombach, K. 2005. Zircon Pb-evaporation ages of granitoids from the Strzegom-Sobótka massif (SW Poland). *Mineralogical Society of Poland, Special Papers*, **25**, 241–245.

Turniak, K., Halas, S. and Wójtowicz, A. 2007. New K-Ar Cooling Ages of Granitoids from the Strzegom-Sobótka Massif, SW Poland. *Geochronometria*, **27**, 5–9.

Turniak, K., Domańska-Siuda, J. and Szuszkiewicz, A. 2011. Monazite from the eastern part of the Strzegom-Sobótka massif: chemical composition and CHIME ages. *Mineralogical Society of Poland, Special Papers*, **38**, 178–179.

Turniak, K., Mazur, S., Domańska-Siuda, J. and Szuszkiewicz, A. 2014. SHRIMP U-Pb zircon dating for granitoids from the Strzegom-Sobótka Massif, SW Poland: Constraints on the initial time of Permo-Mesozoic lithosphere thinning beneath Central Europe. *Lithos*, **208-209**, 415–429.

Vernon, R.H. 1984. Microgranitoid enclaves in granites – globules of hybrid magma quenched in a plutonic environment. *Nature* **309 (5967)**, p. 438.

Vernon, R.H. 1991. Interpretation of microstructures of microgranitoid enclaves. In: Didier, J. and Barbarin, B. (Eds), Enclaves and granite petrology, pp. 277–291. Elsevier; Amsterdam.

Vernon, R.H. 2010. Granites Really Are Magmatic: Using Microstructural Evidence to Refute Some Obstinate Hypotheses. In: Forster, M.A. and Gerald, J.D.F. (Eds), The Science of Microstructure – Part I. *Journal of the Virtual Explorer* https://doi.org/10.3809/jvirtex.2011.00264

Waight, T.E., Dean, A.A., Maas, R. and Nicholls, I.A. 2000. Sr and Nd isotopic investigations towards the origin of feldspar megacrysts in microgranular enclaves in two I-type plutons of the Lachlan Fold Belt, southeast Australia. *Australian Journal of Earth Science*, **47**, 1105–1112.

Wark, D.A. and Miller, C.F. 1993. Accessory mineral behavior during differentiation of a granite suite: monazite, xenotime and zircon in the Sweetwater Wash pluton. *Chemical Geology*, **110**, 49–67.

White, A.J.R., Chappell, B.W. and Wyborn, D. 1999. Application of the restite model to the Deddick granodiorite and its enclaves – a reinterpretation of the observations and data of Maas et al. (1997). *Journal of Petrology*, **40**, 413–421.

Wiebe, R.A. 1968. Plagioclase stratigraphy: A record of magmatic conditions and events in a granite stock. *American Journal of Science*, **266** (8), 690–703.

Wiebe, R.A. and Collins, W.J. 1998. Depositional features and stratigraphic sections in granitic plutons: implications for the emplacement and crystallization of granitic magma. *Journal of Structural Geology*, **20** (9–10), 1273–1289.

Wiebe, R.A., Smith, D., Sturm, M., King, E.M. and Seckler, M.S. 1997. Enclaves in the Cadillac Mountain Granite (Coastal Maine) samples of hybrid magma from the base of the chamber. *Journal of Petrology*, **38**, 393–423.

Wolf, M.B. and London, D. 1985, Incongruent dissolution of REE- and Sr-rich apatite in peraluminous granitic liquids: Differential apatite, monazite, and xenotime solubilities during anatexis. *American Mineralogist*, **80**, 765–775.

Wyllie, P.J., Cox, K.G. and Biggar, G.M. 1962. The Habit of Apatite in Synthetic Systems and Igneous Rocks. *Journal of Petrology*, **3**, 238–243.

Zorpi, M.J., Coulon, C., Orsini, J.-B. and Corcita, C. 1989. Magma mingling, zoning and emplacement in calc-alkaline granitoid plutons. *Tectonophysics*, **157**, 315–329.

Žák, J., Verner K., Sláma, J., Kachlík, V. and Chlupáčová, M. 2013. Multistage magma emplacement and progressive strain accumulation in the shallow – level Krkonoše-Jizera plutonic complex, Bohemian Massif. *Tectonics*, **32**, 1493–1512.

Manuscript submitted: 29th October 2018
Revised version accepted: 15th February 2019